Passive Solar Massive Wall Systems With Fins Attached on the Heated Wall and Without Glazing

E. Bilgen
Ecole Polytechnique,
Box 6079,
City Center,
Montreal, Quebec, H3C 3A7, Canada
e:mail: bilgen@meca.polymtl.ca

Natural convection, radiation and conduction heat transfer in passive solar massive wall systems with fins attached to the heated surface and without glazing is experimentally studied. The system was 0.78 m high, 0.40 m wide, and 0.10 m thick concrete wall with 0.025 m long, 0.004 m thick horizontal fins made as an integral part of it and placed at 0.01 m intervals. A heat source was used to impose a constant heat flux which could be varied from about 200 to 800 W/m^2. Temperatures at various points and heat flux by convection at the back were measured. Using periodicity hypothesis and various assumptions, the wall with fins was also analyzed theoretically. The results indicate that for the case considered, about 35 percent of the heat flux imposed on the finned surface goes through the system and is dissipated at the back. [S0199-6231(00)00701-2]

Introduction

It is well known that massive walls are used in passive solar heating and ventilating systems [1]. To reduce heat losses by convection and infra-red radiation from the warm wall to the environment a glazing system is employed. Depending on the climatic condition, the glazing system may consist of a single or double glass pane. Two problems with this system are the cost and maintenance. It is known that major cost is due to glazing system, which is usually a well manufactured and installed window system on the wall. Although the glazing system is often built hermetically, the air in the channel between the massive wall and the glazing circulates by natural convection and as a result, a thin film of dust forms on the channel surfaces; its cleaning presents a problem. In addition, in favorable conditions, it is known that plants can flourish in the same space between the glazing and the massive wall. If the dwelling air is circulated through the channel to ventilate the massive wall system, the situation becomes worse. These problems may be precluded by eliminating the glazing system (i.e., using a massive *non-ventilating* wall exposed to solar radiation). To reduce heat losses from the warm wall by convection and infra-red radiation, a honeycomb like structure may be integrated to the wall.

Honeycomb structures accompanied by a glazing system are often used in building elements and solar components for additional radiation and convection suppression. In this case, tall and usually vertical enclosures are formed. For example, in systems where horizontal two dimensional fins are used, the enclosure consists of two active long sides, one of which is equipped with conducting fins, and two connecting short sides which are insulated. Depending on the size of the fins, equidistant open micro-cavities are formed that are connected to each other with the channel formed in the tall enclosure [2].

A review of the literature shows that in tall enclosures containing fins attached to one active side forming open micro-cavities with various boundary conditions, there are various studies on combined heat transfer by radiation, convection and conduction [2] and natural convection [3–5]. In similar systems without cover, there are no studies. Exceptions are those numerical and experimental studies on natural convection in a single open cavity without a massive wall [6,7], hence, without considering radiation and conduction.

The purpose of the present investigation is to study experimentally heat transfer in massive wall systems with fins attached on the heated side and without a glazing system.

Experimental Apparatus

A schematic of the apparatus used in the experiments is shown in Fig. 1. The details of a micro-cavity are shown in Fig. 2. The massive wall was made of concrete with fins as integral parts of it. The dimension of the wall was 0.40 m wide, $H=0.78$ m high and $L=0.10$ m thick, excluding fins. Two dimensional fins were 0.40 m wide, $l=0.025$ m long and $e=0.004$ m thick separated from one another by $h'=0.01$ m. Based on the results of the previous studies in tall enclosures [4,5], the dimension of the fins was chosen to obtain an aspect ratio of $A'=h'/l'=0.4$ for the micro-cavities, which is optimal for these systems. Their thickness was dictated by the fabrication possibility using concrete. The back surface of the finned surface was flat. The horizontal and vertical extremities of the wall were insulated by 0.05 m polystyrene insulation substrate.

Thermocouples were attached at three levels, 0.10 m, 0.39 m, and 0.68 m elevation. Details at mid-level (0.39 m elevation) are shown in Fig. 1. The holes were drilled with a mill to ensure accurate location of the temperature measurements. The thermocouples were from fine, 1.27 10^{-3} copper-constantan thermocouples wire and attached with epoxy and later covered with concrete. The ambient air temperature far from the apparatus as well as the air temperatures in the boundary layer at 0.78 m level were measured using platinum probes. The convection heat flux at the back surface was measured using a heat flux meter, the resolution of which was ± 1 W/m^2. The heat flux meter was made of copper with an emissivity $\epsilon=0.05$, hence its radiation was negligibly small, since the surface temperatures were at the same order as that of ambient air. This was examined in a study by altering its surface condition. The flux meter surface was painted with a thin coating using flat black paint. It was seen that the meter indicated, in this case, the combined heat transfer by convection plus radiation, which was verified by theoretical estimates. With this assurance, all experiments were carried out using the flux meter without paint, indicating the heat flux by convection only.

Contributed by the Solar Energy Division of THE AMERICAN SOCIETY OF MECHANICAL ENGINEERS for publication in the ASME JOURNAL OF SOLAR ENERGY ENGINEERING. Manuscript received by the ASME Solar Energy Division, Sept. 1999; final revision Feb. 2000. Associate Technical Editor: M. Olszewski.

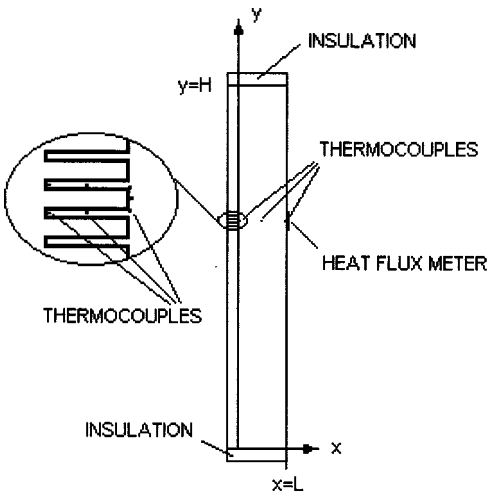

Fig. 1 Schematic of the test apparatus

The heat source was a multiple-lamp design system. 25×75 W halogen light bulbs were installed in a staggered form in an area of 1 m by 1 m. It is known that radiation produced by halogen light bulbs has a spectral distribution similar to solar radiation in the wavelength range of 0.20–2.7 μm, which contain 97 percent of the energy in solar radiation [8]. A rheostatic control was used to provide the desired heat flux for each experiment, which varied from about 200 to 800 W/m^2. The rheostatic set points, which were determined using a voltmeter, were calibrated using a radiometer at the center of the receiving surface level of the apparatus, which was at 1 m distance. The heat flux measurements were made on the receiving surface placed at 1 m, and using a mesh of 0.1 m by 0.1 m for traversing. It was found that at the receiving surface level, the fluctuation of the heat flux was less than ±2.5 percent over the average heat flux on the surface.

The wall and the fins were made of unpainted concrete. Its measured density was 2030 kg/m^3. Thermophysical property data taken from the literature were: thermal capacity c_p=837 J/kg·K, thermal conductivity k=1.0 W/m·K, the emissivity ϵ=0.9. A 0.1 m thick wall made of the same material but without fins was used as a reference apparatus, and using these thermophysical property data, measurements and analysis were carried out for various heat fluxes. They yielded corroborative values within ±1 percent when compared with theoretical calculations. In addition, using the theoretical model explained later, a sensitivity study was carried out with the surface emissivity and thermal conductivity. It was seen that the effect of ϵ when varied from 0.85 to 0.95 (i.e., by ±5.6 percent about the literature data) on the end results was less than ±0.5 percent on T_2, ±0.06 percent on T_4 and ±1 percent on q_{cv}; that of the thermal conductivity when varied from 0.8 to 1.2 (i.e., by ±20 percent about the literature data) was less than ±0.6 percent, ±0.5 percent, and +0.9/−0.1 percent on the same parameters, respectively. Therefore, it was concluded that these property data from the literature could be used without further consideration.

The experiment was carried out in a basement laboratory free of ventilation currents. The working fluid was air. The ambient air temperature varied less than 0.2°C through the experimentation, which took typically 24 hours, which included heating experiment of about 15 hours and cooling of 9 hours. A data logging system consisting of multiplex carts and a P.C. was used to collect data of transient temperatures and heat flux at the back surface. The experimental error in temperature measurements was estimated to be ±2.4°C, which resulted from various sources: compensation error ±1°C, linearization error ±0.03°C, offset error ±0.76°C, thermocouple error ±2°C. The error in heat flux measurement was estimated to be ±1.6 W/m^2, which is based on ±1.1 W/m^2 compensation error, ±0.6 W/m^2 read out instrument error and ±1 W/m^2 heat flux sensitivity.

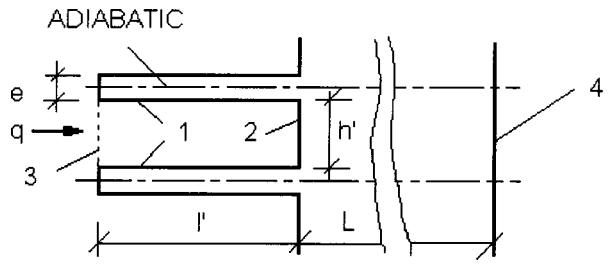

Fig. 2 Schematic of the open micro-cavity

Data Reduction

Experiments were carried out starting from the steady state condition, i.e., the apparatus at the ambient temperature. At the desired heat flux imposed on the system, the experiment was continued until a steady condition was reached, which took about 10 to 15 hours. The steady state temperatures and heat fluxes were then obtained. The aim of the study was to examine at the mid-level elevation, the variation of steady state surface temperatures at the front and the back, the variation of steady state temperatures at various points of the fins and the steady state heat flux by natural convection at the back surface as a function of the imposed heat flux and ambient temperature. These will be presented in appropriate figures, after analyzing the wall with micro-cavities.

Analysis

Previous theoretical results with wall and microcavities in a cavity, hence, with a glazing system, have shown that in tall systems with high number of fins the heat transfer problem could be solved as that in a single micro-cavity using the periodicity hypothesis [4,5]. Therefore, it will be assumed that the periodicity hypothesis holds also in this case and the combined heat transfer will be analyzed in a single micro-cavity shown in Fig. 2. It is noted that due to symmetry, the horizontal boundaries of a microcavity are adiabatic. Further, the experimental results showed that the temperature on various points of the lower and upper fins had a maximum variation of 3.5 percent. Hence, it is assumed that the fins are isothermal with negligible mass and also adiabatic. It is further assumed that (i) surfaces are diffuse and gray; (ii) they have uniform temperatures and radiosities; (iii) surroundings are large and isothermal; (iv) the opening may be considered as a hypothetical surface at the surrounding temperature, T_∞, with an emissivity ϵ=1, since all the radiation incident on the hypothetical surface will be absorbed.

With these assumptions, following energy conservation equations and the heat flow rates by convection, radiation and conduction on surfaces 1, 2, and 4 (see Fig. 2), can be written:

energy balance on surface 2:

$$Q_{in}=Q_{cv2}+Q_{r2}+Q_{c2} \tag{1}$$

where

$$Q_{cv2}=h_2A_2(T_2-T_a) \tag{2}$$

$$Q_{r2}=(E_{b2}-J_2)/((1-\epsilon_2)/(\epsilon_2A_2))$$
$$=(J_2-J_1)/(1/A_2F_{21})+(J_2-J_3)/(1/A_2F_{23}) \tag{3}$$

$$Q_{c2}=(k/L)A_2(T_2-T_4)$$
$$=Q_{cv4}+Q_{r4}$$
$$=h_4A_4(T_4-T_\infty)+\sigma A_4\epsilon_4(T_4^4-T_\infty^4) \quad (4)$$

where the last term is obtained by noting that $A_4/A_{4\infty}\approx 0$ and $F_{4\infty}\approx 1$.

$$Q_{c2}=h_4A_4(T_4-T_a)+h_{r4}A_2(T_4-T_\infty) \quad (5)$$

$$h_{r4}=\sigma A_4\epsilon_4(T_4^2-T_\infty^2)(T_4+T_\infty) \quad (6)$$

$$E_{b1}=\sigma T_1^4 \quad (7)$$

$$E_{b2}=\sigma T_2^4 \quad (8)$$

$$J_3=E_{b3}=\sigma T_3^4 \quad (9)$$

energy balance on adiabatic surface 1:

$$Q_{cv1}+Q_{r1}=h_1A_1(T_1-T_a)+(E_{b1}-J_1)/((1-\epsilon_1)/(\epsilon_1A_1))=0 \quad (10)$$

where

$$Q_{r1}=(E_{b1}-J_1)/((1-\epsilon_1)/(\epsilon_1A_1))$$
$$=(J_1-J_2)/(1/(F_{12}A_1))+(J_1-J_3)/(1/(F_{13}A_1)) \quad (11)$$

Equations (1) to (11) result in a system of simultaneous linear equations of the form [a][x]=[b] with unknowns of T_1, T_2, T_4, J_1 and J_2 in [x].

$$-(A_2F_{21})J_1+(A_2F_{21}+A_2F_{23}+(\epsilon_2/A_2)/(2-\epsilon_2))J_2$$
$$=J_3A_2F_{23}+E_{b2}(\epsilon_2/A_2)/(2-\epsilon_2) \quad (12)$$

$$(h_2A_2+(k/L)A_2)T_2-(k/L)A_2T_4-((\epsilon_2/A_2)/(2-\epsilon_2))J_2$$
$$=Q_{in}-E_{b2}(\epsilon_2/A_2)/(2-\epsilon_2)+h_2A_2T_3 \quad (13)$$

$$(k/L)A_2T_2-((k/L)A_2+h_4A_4+h_{r4}A_4)T_4=-(h_4A_4+h_{r4}A_4)T_3 \quad (14)$$

$$h_1A_1T_1-(\epsilon_1/A_1)/(1-\epsilon_1)J_1=-E_{b1}(\epsilon_1/A_1)/(1-\epsilon_1) \quad (15)$$

$$(2A_1/F_{12}+2F_{13}/A_1+(\epsilon_1/A_1)/(1-\epsilon_1))J_1-(2A_1/F_{12})J_2$$
$$=(E_{b1}(\epsilon_1/A_1)/(1-\epsilon_1)+2J_3F_{13}/A_1) \quad (16)$$

In Eqs. (12)–(16), the view factors, F_{ij}, are evaluated for a two dimensional cavity as $F_{12}=0.405$, $F_{21}=1.029$, $F_{13}=0.405$, and $F_{23}=0.18976$ [9]; h_1, h_2, and h_4 are evaluated using empirical correlations for natural convection. In particular, on the back surface, the correlation of [10] for the whole back surface was used to evaluate h_4. Inside the cavity surfaces, the Rayleigh number varied from about 1500 to 3300 showing that the heat transfer was by a quasi-conduction mode and the empirical correlations for large horizontal and vertical surfaces could not be used. Hence, the convection heat transfer from the horizontal surfaces, h_1, was considered to be by conduction only and for the vertical surface, h_2, the correlation and information of [7] were used.

The simultaneous linear equation system, Eqs. (12)–(16), is solved by a numerical iterative technique. All the parameters in [a] and [b] are known for an applied heat flow rate and through the thermophysical constants. The computational procedure was: compute the convection coefficients, h_1, h_2, and h_4, the radiation coefficient, h_{r4}, E_{b1}, and E_{b2} for initial values $[x_0]$; then, compute new values $[x_n]$, check the convergence condition of $\Delta[x]\leqslant 0.01$ and stop if it is satisfied. If it is not, use the new values $[x_n]$ and repeat the computation procedure until the convergence condition is satisfied.

Results and Discussion

Eight experiments were carried out using heat flux from 200 to 800 W/cm^2 as described earlier. The results are reduced and presented in Figs. 3–6. The theoretical results are also presented in the same figures, which will be discussed in this section.

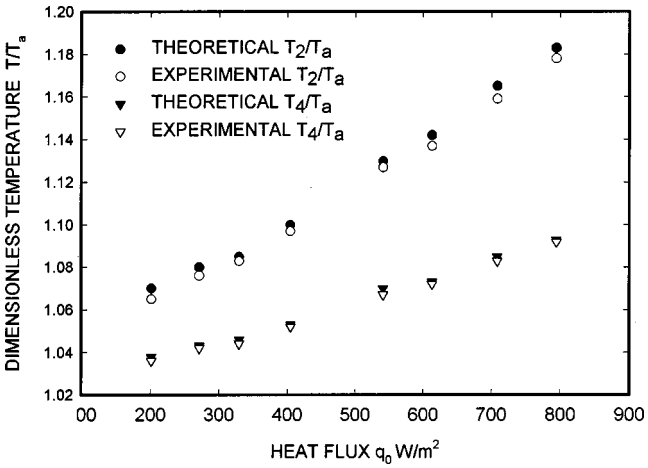

Fig. 3 Experimental and theoretical dimensionless temperatures on surfaces 2 and 4 of Fig. 2 as a function of heat flux imposed on the system

Figure 3 shows dimensionless temperatures, T_2/T_a and T_4/T_a on surfaces 2 and 4 as a function of imposed heat flux, q_0. It should be mentioned that the air temperature, T_a was constant during each experiment but a little different from experiment to experiment, which is taken care of by normalizing the surface temperatures by air temperature. It is observed that the normalized surface temperatures follow almost a linear relationship with the heat flux, although a little non-linearity exists, as it should. The reason is due to small variation of the dimensionless temperature, from about 1.04 to 1.18 only. The theoretical values also plotted show that T_2/T_a is over estimated by about 2 percent, but agreement is much better with T_4/T_a at the back surface. The main reason may be due to simplifications made in simulating heat transfer by natural convection and radiation on the finned surface.

Heat flux by convection on the back surface, q_{cv} as a function of imposed heat flux, q_0, is shown in Fig. 4. The relationship is seen to be almost linear as it was noticed also in Fig. 3 for the surface temperatures. Comparison with the theoretical results show good agreement with the deviation of ± 3 percent, except at the lowest flux, for which the deviation is a little less than 10

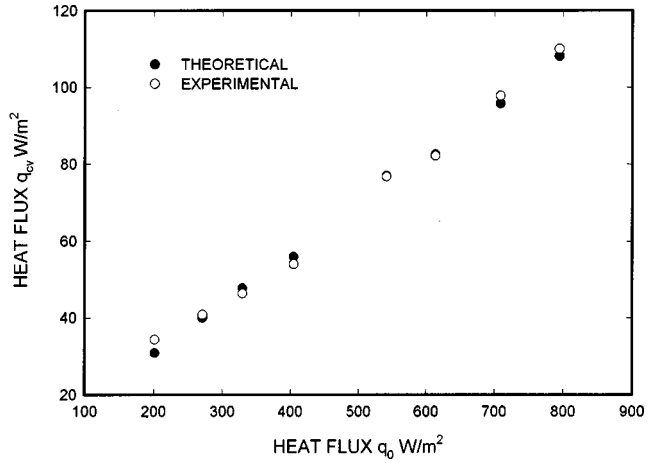

Fig. 4 Experimental and theoretical heat flux by natural convection at the back (surface 4 of Fig. 2) as a function of imposed heat flux on the system

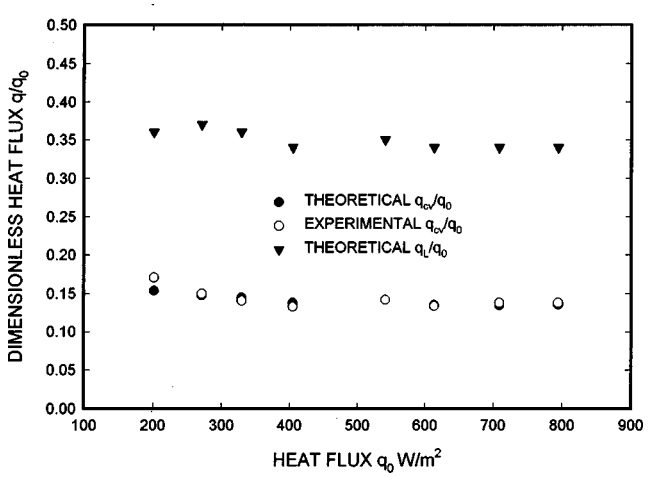

Fig. 5 Experimental and theoretical heat fluxes at the back by natural convection, and theoretical combined heat flux as a function of imposed heat flux on the system

percent. In view of the experimental errors discussed earlier and simplifications made for modeling, the deviation at the lower end is expected.

Heat flux by convection at the back (which was presented in Fig. 4) normalized with imposed heat flux is presented as a function of imposed heat flux in Fig. 5. It is seen that 15 percent of the imposed heat on the system is dissipated by convection at the back. Theoretical results are also shown with the deviations discussed earlier in Fig. 4. Theoretical combined dimensionless heat transfer by natural convection and radiation, q_L/q_0, is also plotted in the same figure, which shows that about 35 percent of the imposed heat flux goes through the system and is dissipated at the back. In a practical situation, for example, for a solar passive wall system, this may represent a thermal efficiency. It should be noted that in practical conditions, the overall thermal performance of solar passive systems using a massive wall has been determined to be at the same order of magnitude. However, in practical conditions, there are other parameters involved, such as wind at the collector surface, low outside temperatures, and variable solar radiation. Therefore, a direct comparison is not possible.

Fractions by heat flux by convection and radiation are calculated and presented in Fig. 6. It is seen that about 35 percent of the heat flux at the back is dissipated by convection and 65 percent by radiation. It seems that these fractions do not vary considerably with the magnitude of the imposed heat flux on the system.

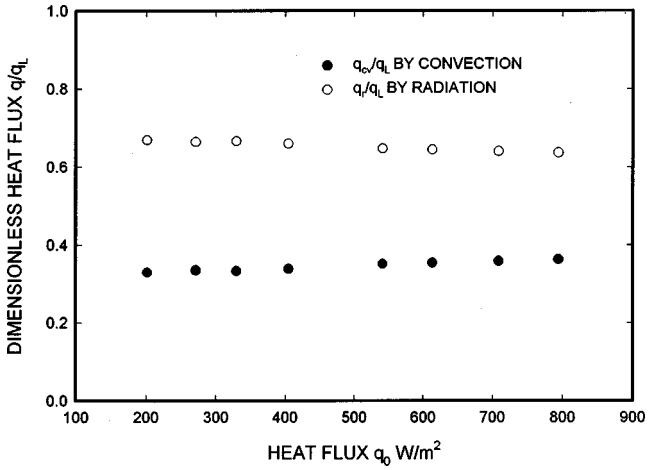

Fig. 6 Fraction of heat transfer by convection and radiation at the back (surface 4 of Fig. 2) as a function of the imposed heat flux on the system

Conclusions

Heat transfer by natural convection, conduction, and radiation has been studied experimentally in massive wall systems with fins attached on heated side. By using periodicity hypothesis and various assumptions, the wall with fins is modeled as a system consisting of open micro-cavities attached to a massive wall. For the case considered, the results showed that i) heat flux by natural convection at the back of the wall increased almost linearly with increasing heat flux applied on the finned surface; ii) nondimensional heat flux by natural convection at the back of the wall, q_{cv}/q_0, was almost constant at around 15 percent when plotted as a function of the heat flux applied at the finned surface; iii) similarly, the theoretical combined heat transfer at the back was almost constant, at around 35 percent; the fractions of natural convection and radiation were about 35 and 65 percent, respectively.

In the light of these findings, it is concluded that to reduce cost and maintenance, massive walls with fins attached to heated surface may be used for solar passive systems and building components, with satisfactory thermal performances. The experimental results and the theoretical analysis of this study may be used in preliminary studies and designs of passive systems to determine suitable geometry for a given application.

Acknowledgments

Financial support by Natural Sciences and Engineering Research Council of Canada is acknowledged. The experimental study and data collection were carried out by Mr. Ludovic Megne Ndong.

Nomenclature

A = area, m^2
A' = micro-cavity aspect ratio, h'/l'
$[a]$ = coefficient matrix
$[b]$ = right hand side vector
c_p = thermal capacity, J/kg·K
E_b = black body emissive power, W/m^2
e = fin thickness, m
l' = fin length, m
F_{ij} = view factor
h' = height of the micro-cavity, m
h = average heat transfer coefficient, $W/m^2 \cdot K$
H = total height of the system, m
J = radiosity, W/m^2
L = wall thickness, m
Q = heat flow rate, W
q = heat flux, W/m^2
Ra = Rayleigh number, $(g\beta\Delta TH^3)/(\nu\alpha)$
T = temperature, K
T = dimension temperature, T_i/T_a
T_∞ = temperature of surrounding surfaces, K
T_a = temperature of surrounding air, K
$[x]$ = vector of unknown parameters

Greek Symbols

α = thermal diffusivity, m^2/s
β = Volumetric coefficient of thermal expansion, 1/K
ϵ = emissivity
ν = kinematic viscosity, m^2/s
ρ = fluid density, kg/m^2
σ = Stefan-Bolzmann constant, 5.67×10^{-8} $W/m^2 \cdot K^4$

Subscripts

a = air
b = black body

c = conduction
cv = convection
in = in, imposed
L = combined transfer by convection and radiation
r = radiation
1 = micro-cavity horizontal surfaces
2 = micro-cavity vertical surface
3 = micro-cavity opening surface
4 = back surface of the micro-cavity

References

[1] Bilgen, E., and Michel, J., 1979, ''Integration of Solar Systems in Architectural and Urban Design,'' in *Solar Energy Application in Buildings*, ed. A. A. Sayigh, Chap. 9, Academic Press, New York.

[2] Zrikem, Z., and Bilgen, E., 1986, ''Theoretical Study of a Non-Convective Trombe Wall Collector With Honeycomb Structure,'' J. Solar Wind Technol., **3**, pp. 33–44.

[3] Hasnaoui, M., Zrikem, Z., Vasseur, P., and Bilgen, E., 1990, ''Radiation Induced Natural Convection in Enclosures with Conducting Walls,'' J. Solar Wind Technol., **7**, No. 5, pp. 515–525.

[4] Hasnaoui, M., Vasseur, P., and Bilgen, E., 1992, ''Natural Convection in Rectangular Enclosures With Adiabatic Fins Attached on the Heated Wall,'' Wärme und Stoffübertragung, **27**, pp. 357–368.

[5] Lakhal, E. K., Bilgen, E., and Vasseur, P., 1995, ''Natural Convection and Conduction in Massive Wall Solar Collectors With Honeycomb and Without Vents,'' ASME J. Sol. Energy Eng., **117**, pp. 173–180.

[6] Penot, F., 1982, ''Numerical Calculation of Two-Dimensional Natural Convection in Isothermal Open Cavities,'' Numer. Heat Transf., **5**, pp. 421–437.

[7] Chan, Y. L., and Tien, C. L., 1985, ''A Numerical Study of Two-Dimensional Natural Convection in Square Open Cavities,'' Numer. Heat Transf., **8**, pp. 65–80.

[8] Kenny, S. P., and Davidson, J. H., 1994, ''Design of a Multiple-Lamp Large-Scale Solar Simulator,'' ASME J. Sol. Energy Eng., **116**, pp. 200–205.

[9] Siegel, R., and Howell, J. R., 1981, *Thermal Radiation Heat Transfer*, McGraw-Hill, New York.

[10] Churchill, S. W., and Chu, H. H. S., 1975, ''Correlating Equations for Laminar and Turbulent Free Convection From a Vertical Plate,'' Int. J. Heat Mass Transf., **18**, pp. 1323–1329.